

Synthesis of high payload nanohydrogels for the encapsulation of hydrophilic molecules via inverse miniemulsion polymerization: caffeine as a case study

*Original*

Synthesis of high payload nanohydrogels for the encapsulation of hydrophilic molecules via inverse miniemulsion polymerization: caffeine as a case study / Artusio, F.; Ferri, A.; Gigante, V.; Massella, D.; Mazzarino, I.; Sangermano, M.; Barresi, A. A.; Pisano, R.. - In: DRUG DEVELOPMENT AND INDUSTRIAL PHARMACY. - ISSN 0363-9045. - STAMPA. - 45:12(2019), pp. 1862-1870. [10.1080/03639045.2019.1672714]

*Availability:*

This version is available at: 11583/2764492 since: 2020-02-22T17:51:10Z

*Publisher:*

TAYLOR & FRANCIS INC

*Published*

DOI:10.1080/03639045.2019.1672714

*Terms of use:*

This article is made available under terms and conditions as specified in the corresponding bibliographic description in the repository

*Publisher copyright*

Taylor and Francis postprint/Author's Accepted Manuscript

This is an Accepted Manuscript of an article published by Taylor & Francis in DRUG DEVELOPMENT AND INDUSTRIAL PHARMACY on 2019, available at <http://www.tandfonline.com/10.1080/03639045.2019.1672714>

(Article begins on next page)



## Synthesis of high payload nanohydrogels for the encapsulation of hydrophilic molecules via inverse miniemulsion polymerization: caffeine as a case study

Fiora Artusio, Ada Ferri, Valeria Gigante, Daniele Massella, Italo Mazzarino, Marco Sangermano, Antonello Barresi & Roberto Pisano

To cite this article: Fiora Artusio, Ada Ferri, Valeria Gigante, Daniele Massella, Italo Mazzarino, Marco Sangermano, Antonello Barresi & Roberto Pisano (2019): Synthesis of high payload nanohydrogels for the encapsulation of hydrophilic molecules via inverse miniemulsion polymerization: caffeine as a case study, Drug Development and Industrial Pharmacy

To link to this article: <https://doi.org/10.1080/03639045.2019.1672714>



Accepted author version posted online: 24 Sep 2019.



Submit your article to this journal [↗](#)



View related articles [↗](#)



View Crossmark data [↗](#)

**Synthesis of high payload nanohydrogels for the encapsulation of  
hydrophilic molecules via inverse miniemulsion polymerization:  
caffeine as a case study**

*Fiora Artusio<sup>1</sup>, Ada Ferri<sup>1</sup>, Valeria Gigante<sup>1</sup>*

*Daniele Massella<sup>1</sup>, Italo Mazzarino<sup>1</sup>, Marco Sangermano<sup>1</sup>, Antonello Barresi<sup>1</sup>,*

*Roberto Pisano<sup>1\*</sup>*

<sup>1</sup> Department of Applied Science and Technology, Politecnico di Torino, corso Duca degli

Abruzzi 24, 10129 Torino, Italy

KEYWORDS: hydrogel, nanoparticle, miniemulsion, UV polymerization, caffeine, drug release

## ABSTRACT

The association of an active principle with a nanocarrier is known to improve its stability and protect it from external factors. Nevertheless, loading of nanoparticles with highly hydrophilic substances like caffeine remains a tricky issue. In the present study, inverse miniemulsion systems were successfully coupled to UV radiation to synthesize polymeric nanohydrogels for drug delivery. The proper choice of the continuous and dispersed phase chemical composition led to the entrapment of active principle into the miniemulsion droplets. Our confinement-based strategy enabled unprecedented caffeine encapsulation efficiency inside 100-nm particles. Dimensional, thermal and spectroscopic characterizations were carried out to investigate both unloaded and loaded nanohydrogels. Furthermore, *in vitro* release studies evaluated caffeine release kinetics from nanohydrogels by means of dialysis tests. It was demonstrated that controlled and sustained release occurred within the first 50 hours. Experimental data were found to fit the Higuchi model suggesting that the active principle release is diffusion-controlled.

## INTRODUCTION

Miniemulsion polymerization is nowadays a reliable method for the synthesis of a variety of nano-sized devices, such as bulky or porous particles [1,2] and nanocapsules [3,4]. One of the outstanding features of such a system is represented by the possibility to confine some chemical species within a specific phase. For example, thanks to the immiscibility of the continuous and the dispersed phase, one can restrict a monomer and/or a specific ingredient to the miniemulsion droplets. Then, a solid polymeric envelopment around the drops can be obtained by UV-induced or thermal polymerization. In the present study, this feature has been exploited for the synthesis of nanohydrogels intended for the enhancement of the loading of hydrophilic compounds.

The popularity of hydrogels is increasing thanks to their versatility and biocompatibility. Their high water content, which could overcome their dry weight by thousands of times [5], and their polymeric nature enabled disparate applications reported in literature. Among them one can find soil water retention [6], drug delivery, tissue engineering [7] and cellular immobilization [8]. Generally, hydrogels can be identified as natural or synthetic with respect to the source of the material involved in their synthesis. In both cases, the final structure is represented by a 3D network built up by chemical or physical interactions. If such a structure is replicated at the nanoscale, specific vectors for the delivery of oligonucleotides, DNA [9], hormones, vaccines, immunomodulatory agents [10] and small molecule drugs [11] can be produced. Nanohydrogels provide a valuable platform for the enhancement of drug bioavailability, targeting and life span in circulation [12]. Particular attention has to be paid to the nanocarrier size, which depends on its specific application. For example, it has been demonstrated that particles size affects the probability to cross the blood brain barrier [13], as well as extravasation processes [14] and *in vitro* permeation through rat skin and intestine [15]. In addition, the cutaneous distribution also appears to be governed by the size of polymeric nanoparticles [16].

More specifically, our goal was to synthesize nanohydrogels by means of UV polymerization carried out in a water-in-oil (W/O), or inverse, miniemulsion. Two of the outstanding differences of miniemulsions

from conventional emulsions regard their droplets size and mechanism of nucleation when a polymerization is carried out in such a system. A miniemulsion is characterized by droplets whose size belongs to the nanoscale, typically from 20 to 200 nm, and represents a thermodynamically unstable configuration. Because of this feature, the miniemulsion formation cannot occur spontaneously and an energy input deriving from mechanical devices or particular phase transitions of the components are required [17,18]. When a polymerization is initiated, the particle nucleation is generally dominated by micellar and homogeneous nucleation in emulsion-based systems. Conversely, as far as miniemulsions are concerned, droplet nucleation becomes the leading mechanism since micelles are sacrificed for the stabilization of the significantly higher interface area between continuous and dispersed phase. This feature enables the preservation of droplet size throughout the polymerization process [19].

Caffeine was chosen as the model compound because of its widespread application and chemical nature. As a matter of fact, caffeine is largely employed in food, pharmaceuticals, cosmetics and supplements. Its beneficial effects include increase of mental alertness, enhancement of sport performance, help in weight loss [20,21], treatment for apnea of prematurity [22] and antioxidant activity [23]. This active ingredient could also play a significant role in the inhibition of skin carcinogenesis [24–26]. Notwithstanding the wide range of therapeutic effects of caffeine, its marked hydrophilicity makes its effective administration quite challenging. The enteral administration route results in fast and uncontrolled release, the clearance in the stomach and concentration peaks in blood circulation are reached in about 1 minute, whereas the drug is completely metabolized in about 2-3 hours; therefore, regular administrations are required [27,28]. As regards the dermatological administration, a significant limitation consists in the scarce affinity of caffeine with the lipophilic outer layer of skin, namely the *stratum corneum*; such differences in chemical nature make it difficult to administer a therapeutically effective dosage of caffeine (and in general hydrophilic drugs) at transdermal level [29,30].

Recently, the novelties introduced by nanocarriers for drug encapsulation and controlled release have arisen significant interest in developing caffeine nanoformulations for food and pharmaceutical applications. However, difficulties in achieving very high caffeine encapsulation efficiency (EE) inside

different kinds of nanoparticle have been noticed in literature. For example, EEs were found to be 34% for phosphatidylcholine liposomes [31] and around 80% for nanoparticles obtained from propyl-starch derivatives [32]. Caffeine payloads corresponding to 75% have been reported for solid lipid nanoparticles [33]. Recently, high EEs for both caffeine and lipophilic compounds have been reported for lactoferrin-glycomacropeptide nanohydrogels [34]. As regards percutaneous release of caffeine, microemulsions were investigated as trial formulations and approximately 27% of the applied dose turned out to penetrate the skin in Franz diffusion cell tests [35]. In addition, our previous research [36,37] enquired a productive and scalable approach based on flash nanoprecipitation to load hydrophilic substances in polymeric nanoparticles for transdermal application, evidencing that the higher the drug hydrophilicity, the lower the performances in terms of encapsulation efficiency. Conversely, as regards micrometric systems, microhydrogels produced by means of electrospray led to EEs from 37% up to 65% [38]. EEs ranging from 70% to 85% are reported for alginate and peptide microparticles [39,40], whereas microencapsulation involving polysaccharides led to even higher EEs [41]. Therefore, caffeine represented a challenging molecule to be encapsulated inside nanocarriers and a good benchmark for testing the validity of our system.

This paper presents the synthesis of nanohydrogels by means of miniemulsion UV-triggered polymerization and evaluates the release of a hydrophilic active principle, namely caffeine, from their matrix. Thanks to the initial confinement of caffeine inside miniemulsion droplets and successive *in-situ* polymerization, we achieved high payloads of active principle inside the carrier. To the best of our knowledge, this is the first study presenting unitary encapsulation efficiency of caffeine inside nanohydrogels. Great attention has been paid to the set-up of the synthesis of nanohydrogels in terms of formulation and operating conditions and to the characterization of the product. The loading of caffeine within the carrier has been proved and its release ability has been investigated by means of *in vitro* dialysis tests. The results pointed out the effectiveness of our biocompatible formulation in ensuring high active principle payload and guaranteeing its release over several days.

## MATERIALS AND METHODS

All the chemicals were reagent grade and used as received. Poly(ethylene glycol)diacrylate (PEGDA, MW=700, assay 98%), Span 80, sodium dodecyl sulfate (SDS, assay  $\geq 98.5\%$ ) and caffeine (assay 99%) were obtained from Sigma-Aldrich (Cesano Maderno, Italy), whereas Darocur 1173 and Pluronic PE6100 were obtained from Ciba Specialty Chemical (Hawthorne, NY, USA) and BASF (Ludwigshafen, Germany) respectively. Sunflower oil was purchased from a local grocery store (Simply, Torino, Italy) and water for injections was employed (B. Braun, Milan, Italy).

### *Synthesis of polymeric nanohydrogels*

The synthesis of polymeric nanohydrogels was carried out in inverse miniemulsion by means of UV polymerization. All the operations were carried out at room temperature. Firstly, two separate phases were prepared. The continuous one was made of 75 ml of sunflower oil and surfactant. The dispersed phase consisted of water suitable for injection, monomer (PEGDA, 10 wt% relative to water), photoinitiator (2 wt% relative to monomer) and, when mentioned, caffeine (25 mg/mL). The nanohydrogel synthesis was optimized both in terms of formulation composition and process operating conditions. Firstly, the type and amount of surfactant and the ratio between dispersed and continuous phase were explored in terms of system stability and particle size. Several surfactants were tested, namely SDS, Span 80 and Pluronic PE 6100 and concentration ranged from 0.2 wt% to 0.6 wt% referred to oil. Surfactant was selected according to its ability of properly stabilizing the miniemulsion and a typical synthesis involved the use of 0.4 wt% of Pluronic PE 6100. The volume fraction of the dispersed phase on the continuous one was varied from 0.25 to 1% and the selected one was 1%. After the identification of the optimized formulation, the emulsification step was investigated. We tested two different approaches. The first one involved the addition of the dispersed phase to the continuous one and vigorously stirring for 10 min in order to get a coarse emulsion. This step was followed by the exposure to ultrasounds for 10 min to reduce the size of the droplets and thus obtain a miniemulsion (US, Bandelin,

Sonorex, Germany). However, as it will be discussed later, this technique did not lead to dimensionally uniform miniemulsion droplets. Alternatively, the two phases were mixed together by using a rotor-stator homogenizer (Ultra Turrax T25, IKA, Germany). Rotor speed was varied between 7000 and 14000 rpm and homogenization time was 5 or 10 min. During the homogenization step, particular care was taken in order to avoid the entrapment of excessive air inside the liquid. This was done by continuously fluxing nitrogen in order to avoid the oxygen inhibition of the successive radical UV polymerization. After the mechanical energy input step, a three-necked round bottom flask was loaded with the freshly prepared miniemulsion. A mercury spot-light source lamp (LC8, Hammamatsu, Japan) was inserted into the reactor and this was covered with an aluminum foil to avoid the radiation dispersion. UV exposure time ranged from 5 to 20 min. A gentle mechanical stirring and nitrogen flux were ensured throughout the whole duration of the UV exposure. All the experiments were performed in triplicate.

### *Dimensional characterization*

Dimensional characterization was carried out by means of Dynamic Light Scattering (DLS, Zetasizer NANO ZS90, Malvern, Worcestershire, UK). A preliminary check on pristine sunflower oil was performed. This was done in order to exclude the presence of foreign scattering particles inside the oil. In a typical analysis, 1 mL of polymeric nanohydrogel suspension was withdrawn from the reactor after the polymerization and then inserted into a disposable polystyrene cuvette. This was then fitted inside the instrument chamber. All the measurements were performed at 25 °C and the scattering angle was 90°. The resulting Z-average and polydispersity index (PDI) values emerged from three measurements per sample. One-way ANOVA analyses were carried out to check data statistical significance by means of Minitab 17. Conventional p-value < 0.05 was assumed as threshold to assess whether process parameters had a significant effect on nanohydrogel size and PDI.

### *Thermal analyses*

Differential Scanning Calorimetry (DSC Q200, TA Instruments, New Castle, DE, USA) was used to investigate the thermal behavior of the product. 12 mL of nanohydrogel suspension were withdrawn from the reactor and transferred into a Falcon tube. Centrifugation was carried out at 15800 g for 15 min (ThermoScientific SL16, Osterode, Germany) in order to separate the polymeric nanohydrogels from the oily continuous phase. Then, the solid residue was transferred into a polystyrene boat and left drying at room temperature for four days. Particular care was taken to remove as much as possible residual oil from the sample with a filter paper. All these preliminary operations were conceived to remove the material, such as water, whose thermal transitions would disturb the detection of monomer and polymer thermal transformations. Sample mass between 10 and 15 mg was loaded into an aluminum pan (TZERO pan, TA Instruments, New Castle, DE, USA). The DSC experiment initial temperature was -80°C, the heating ramp was set at 5 °C/min and the final temperature was 150 °C. A constant nitrogen flux of 50 mL/min guaranteed an inert atmosphere inside the chamber for the whole duration of the measurement.

### *FT-IR investigation*

Samples were prepared according to the above presented drying procedure. A Fourier Transformed InfraRed spectrometer operated in Attenuated Total Reflectance mode (FT-IR ATR, Nicolet iS50, Thermo Scientific, Waltham, MA, USA) was used to investigate the chemical nature of the polymeric material. The instrument was equipped with a Smart ITX diamond. FTIR spectra were collected between 600 and 4000  $\text{cm}^{-1}$  with 4  $\text{cm}^{-1}$  resolution. Each sample was scanned 64 times to collect the final spectrum. In addition, to confirm our assumption of unitary encapsulation efficiency, 12 mL of nanohydrogels suspension were withdrawn from the reactor immediately after polymerization and centrifuged at 15800 g for 15 min so as to separate the nanohydrogels from the oil. The supernatant was collected and analyzed in order to confirm the absence of caffeine traces in the continuous oily phase.

### *In vitro release tests*

In vitro release studies of caffeine from nanohydrogels were performed by setting up dialysis tests. For this purpose, dialysis tubing cellulose membranes (molecular weight cut-off = 14000 Da, Sigma-Aldrich, Cesano Maderno, Italy) were selected and pre-conditioned in phosphate-buffered saline (PBS, pH = 7.4) for 10 min. The total amount of a freshly prepared suspension of caffeine-loaded nanohydrogels was transferred into the dialysis bag and the system was dipped into 1.5 L of PBS. Because of our confinement-based synthesis set-up, the total amount of caffeine loaded into the nanohydrogel suspension can be calculated *a priori* since the caffeine concentration and the volume of the dispersed phase are set during the synthesis. Therefore, the loaded mass of caffeine is equal to 17.1 mg. The system was kept under low magnetic stirring for the whole release duration and covered with a lid so as to limit water evaporation. 5 mL of solution were withdrawn from the receptor compartment and replaced by the same amount of PBS solution in order to keep the same volume of liquid throughout the experiment. Samples were collected every hour for the first 50 hours and then sampling frequency was lowered. The caffeine release was monitored for 9 days. A further control release test was performed on a non-encapsulated caffeine formulation. Briefly, the dispersed phase was made of drug and water, whereas the continuous one included oil and surfactant. The two phases were formulated according to the same ratios used in the first release experiment, except for the absence of monomer and photoinitiator. The emulsion was created by means of Ultra Turrax mixing and was irradiated with UV light. The solutions were transferred into disposable polystyrene UV-transparent cuvettes and analyzed by means of a UV/VIS spectrophotometer (Jenway 6850, Bibby Scientific, Stone, UK). Blank was collected on PBS. The caffeine absorbance values were measured at 273 nm, thus enabling the calculation of caffeine concentration by means of Lambert-Beer law, as reported by previous studies [42]. The data corresponding to the sustained release of caffeine, before the plateau, were then fitted with different kinetic models in order to disclose and evaluate the release mechanism. The tested models were: Zero-Order, First-Order, Higuchi, Hixson-

Crowell and Baker-Lonsdale. As a comparison, the whole set of data was fitted with a Weibull function whose general form is:

$$\frac{m_{c,\text{caffeine}}(t)}{m_{c,\text{caffeine}}(\infty)} = F(t) = 1 - \exp(-at^b) \quad (1)$$

where  $m_{c,\text{caffeine}}(t)$  and  $m_{c,\text{caffeine}}(\infty)$  are the cumulative mass of caffeine at time  $t$  and infinite time respectively.  $F(t)$  is the cumulative fraction of released caffeine and  $a$  and  $b$  are two fitting parameters [43]. All the dialysis tests were performed in triplicate to ensure reproducibility.

## RESULTS AND DISCUSSION

### *Synthesis and characterization of the polymeric carrier*

UV polymerization in miniemulsion represents a valuable tool to synthesize nanoparticles. In particular, this technique is here applied to an inverse miniemulsion whose droplets are made of water, monomer and photoinitiator. The continuous phase is composed of sunflower oil and surfactant. Such a system can be considered as the template of the final nanoparticle suspension since polymerization is confined inside each droplet and does not alter their dimension, provided that the dispersed phase is properly stabilized throughout the reaction. As a matter of fact, thanks to the choice of two immiscible phases and an effective surfactant, diffusion of reactive species outside the polymerizing drops is hindered and size is preserved. Therefore, the initial step of our study involved the identification of the template optimal composition and set of operating conditions, namely those concerning emulsification and polymerization steps.

Particular attention was devoted to the preliminary identification of two immiscible solvents which represent the continuous and the dispersed phase. Taking into account biocompatibility and non-toxicity

requirements deriving from the final drug delivery application of the nanohydrogels, sunflower oil and water for injections were selected. The former represents a natural and low-cost compound which is known for being a valuable penetration enhancer for transdermal release of drugs, thus facilitating their delivery throughout the skin. The latter has been chosen in order to ensure that the solubility of our model active principle, namely caffeine, would not be altered by the presence of ionic species. In addition, this emulsion chemical composition enabled the confinement of the monomer (PEGDA) and the photoinitiator (Darocur 1173) to the aqueous dispersed phase. A representation of the experimental set-up is depicted in Figure 1. Because of its architecture, the system is suitable for the encapsulation of hydrophilic compounds. Moreover, the final product is a vegetable oil-based suspension of nanohydrogels, which could be suitable for potential application to transdermal delivery of drugs.

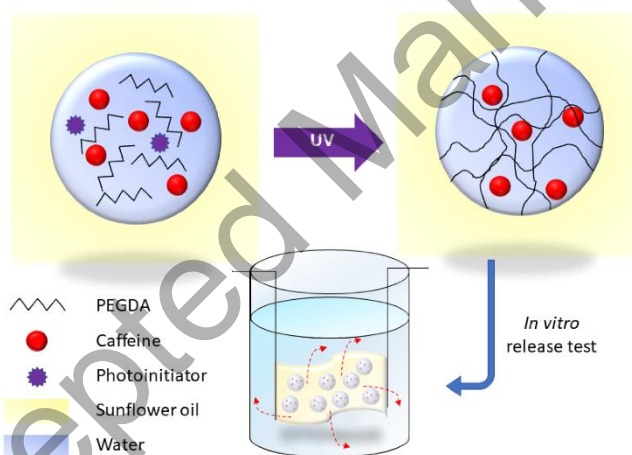


**Figure 1.** Schematic representation of the experimental set-up of the present study. Droplets made of an aqueous solution of monomer, photoinitiator and active principle are polymerized thanks to UV light exposure. This suspension of nanohydrogels is then tested in terms of caffeine release kinetics.

A critical step was represented by the choice of an efficient surfactant system so as to stabilize the newly formed interface after the emulsification step and to avoid Ostwald ripening and/or coalescence of the

droplets by collision. As a matter of fact, achieving a monodisperse nanohydrogel population and limiting aggregation both require stability of the miniemulsion throughout the whole polymerization step. For this purpose, both ionic, such as SDS, and non-ionic surfactants, such as Span 80 and Pluronic PE 6100, were tested. Preliminary tests were conducted with 0.2 wt% of surfactant referring to the continuous phase, following our previous work on miniemulsion-based synthesis of nanoparticles [3]. However, different locations based on surfactant preferential solubility were selected: Span 80 was added to the oil, whereas SDS was dissolved in water. As expected, the non-ionic surfactant Span 80, whose hydrophilic-lipophilic balance (HLB) is far lower than that of ionic ones, provided better stabilization of the drops after the mechanical energy input step compared to SDS. The use of SDS resulted in excessive foaming during the dispersed phase preparation and uncontrolled aggregation among nanoparticles after polymerization, confirming its inadequacy in leading to a stable inverse miniemulsion. By contrast, in general, Span 80 led to the formation of miniemulsions characterized by improved stability. The average size of the nanoparticles obtained with Span 80 was 170 nm, but the standard deviation and the polydispersity index turned out to be unacceptably high. Moreover, after a few hours from polymerization, the samples turned out to be unstable and aggregation occurred. To solve this issue, the surfactant concentration was increased and a better-performing non-ionic surfactant was tested in the following part of the study. Guaranteeing miniemulsion stability is an extremely important feature since, if the formation of coagulum occurs or droplets are coalescing during UV irradiation, the polymerization outcome will be a polydispersed system without defined quality attributes. In order to preserve droplet size throughout the UV exposure, three ratios of Pluronic were tested and, the average nanoparticle diameter and polydispersity index (PDI) are reported in Table 1. Ratios equal to 0.6 wt% overcame the solubility of Pluronic in oil and were excluded. Ratios equal to 0.3 and 0.4 wt% led to the formation of improved quality emulsions which were successively polymerized for 15 minutes. The highest amount of surfactant (0.4 wt%) was responsible for the formation of smaller particles with lower standard deviations and was adopted for the following experiments. Such a formulation will be addressed as the optimized one from here on out.

**Table 1.** Nanoparticle average size, standard deviation (std dev) and PDI as measured by DLS. In all the runs, the emulsion was sonicated for 10 min and exposed to UV radiation for 15 min.

<i>Surfactant</i>	<i>Surfactant, wt %</i>	<i>Z-Average, nm</i>	<i>Std dev, nm</i>	<i>PDI, -</i>
<i>Span 80</i>	0.2	170.0	69.5	0.69
<i>Pluronic PE 6100</i>	0.3	245.2	30.5	0.19
<i>Pluronic PE 6100</i>	0.4	176.6	13.4	0.29

However, it was observed that ultrasound exposure was not efficient for emulsification. The resulting miniemulsion did not possess the necessary uniformity in order to be considered as a proper template for particle production. Moreover, as the continuous phase is made of sunflower oil, its rather high viscosity, compared to that of water, could be responsible for inefficient exploitation of the cavitation processes for droplet breakage. In the perspective of optimization of the mechanical energy input and scalability, a high shear device, namely Ultra Turrax (UT), was selected as an alternative method for the dispersion of the two phases. Preliminary tests were carried out to set homogenization time and speed; results are reported in Table 2.

**Table 2.** Nanoparticle average size and PDI as measured by DLS for the homogenization step study. All the runs were carried out using the optimized formulation which had been exposed to UV radiation for 15 min.

<i>Homogenization speed, rpm</i>	<i>Homogenization time, min</i>	<i>Z-Average, nm</i>	<i>Std dev, nm</i>	<i>PDI, -</i>
7000	5	Insufficient		
7000	10	Insufficient		
14000	5	189	8.7	0.26
14000	10	116	5.2	0.28

Homogenization speed equal to 7000 rpm was not sufficient for the formation of the miniemulsion for neither 5 or 10 min of processing. Increasing UT speed up to 14000 rpm was beneficial and provided the necessary amount of mechanical energy to disperse the aqueous phase in the oily one. Uniform W/O miniemulsions were achieved and the effect of UT time on the final size of particles was elucidated by polymerizing the samples and performing DLS analyses. Increasing UT time led to significantly smaller nanohydrogels, as evidenced by ANOVA ( $p=0.000$ ). On the other side, it did not significantly affect the sample polydispersity ( $p = 0.741$ ). Therefore, homogenization parameters were set at 14000 rpm and 10 min since they enabled the achievement of the desired nanohydrogel size.

Further investigation was carried out to set the proper UV irradiation time and, consequently, get the polymeric network. UV exposure ranged from 5 to 25 min, but, up to 10 min, monomer crosslinking was not effective. As a matter of fact, insufficient exposure caused the formation of a liquid coagulum after some days, indicating that polymerization was not completed. This hypothesis was confirmed by means of thermal analysis of the irradiated samples by DSC. Thermograms were compared to those of pristine

sunflower oil and PEGDA, reported in the Supporting Information (Figure S1 and S2 respectively). The former was characterized by strong endothermic melting peaks in the  $-40\text{ }^{\circ}\text{C} - 0\text{ }^{\circ}\text{C}$  region, whereas the latter displayed the typical melting peak of PEGDA between  $12\text{ }^{\circ}\text{C}$  and  $17\text{ }^{\circ}\text{C}$ . Such peaks were taken as reference for the presence of residual oil and unconverted monomer in the dried samples, obtained according to the procedure previously described. DSC thermograms of the samples irradiated for 10 and 15 min are depicted in Figure 2.

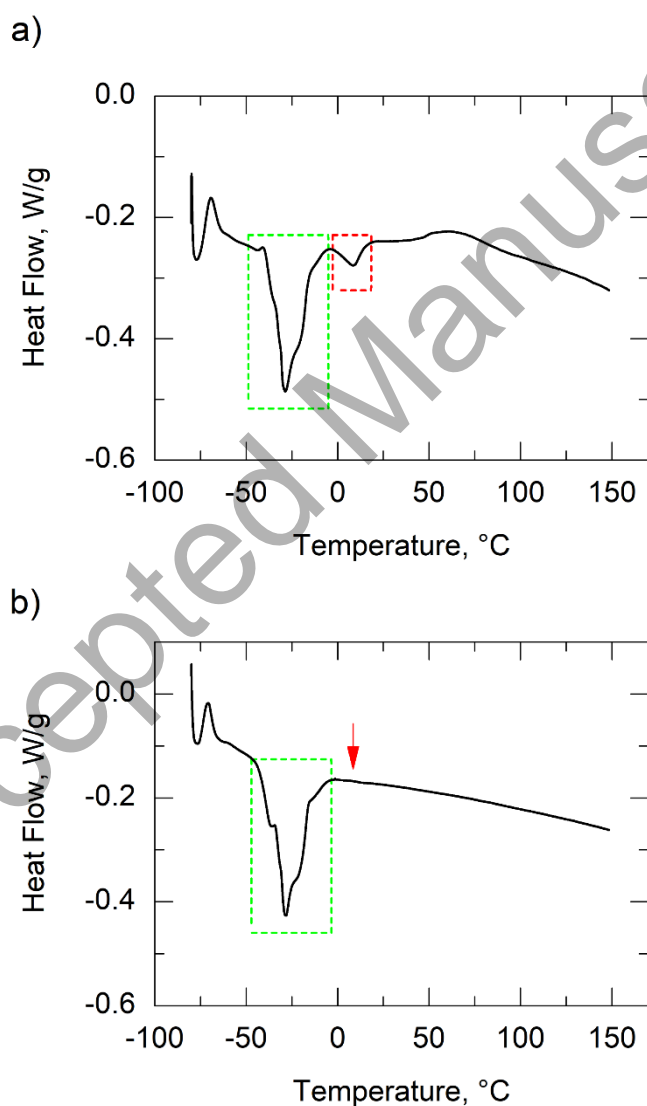


**Figure 2.** a) DSC of the sample irradiated for 10 min. Sunflower oil and unconverted monomer melting are highlighted by the green and red dotted boxes respectively. b) DSC of the sample irradiated for 15

min. There is no residual monomer melting (the corresponding region is indicated by the red arrow). Residual sunflower oil melting is highlighted by the green box. Samples were prepared according to the optimized formulation. UT speed and time were 14000 rpm and 10 min respectively.

The comparison between the two curves provided evidence for the dramatic impact of UV exposure time on the formation of the nanohydrogel network. Samples irradiated for less than 10 min showed the typical thermal behavior illustrated in Figure 2a. In particular, unconverted PEGDA resulted in the appearance of its melting peak between 12 and 17 °C. By contrast, when longer irradiation times were set, the curve significantly changed and the monomer melting peak was missing. Further evidence for the effective monomer crosslinking was provided by the FTIR-ATR characterization of the sample irradiated for 15 min, shown in Figure 3.

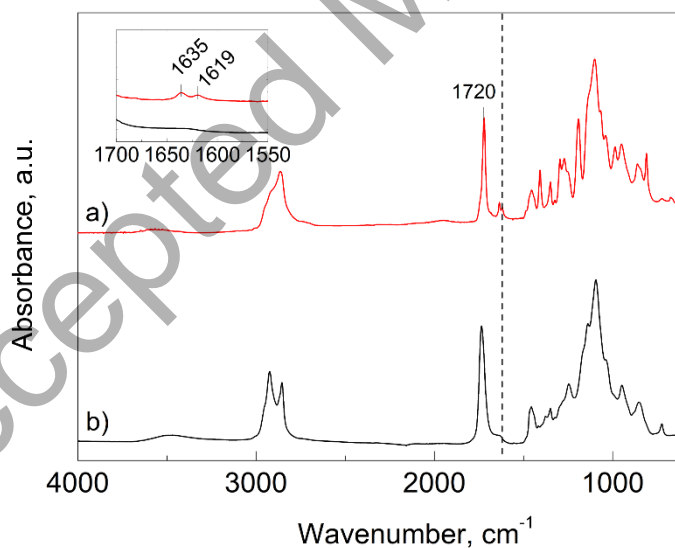


**Figure 3.** FTIR-ATR spectra of a) pristine PEGDA and b) polymerized nanohydrogels. The zoom on the 1700-1500 cm<sup>-1</sup> area is embedded. UT speed and time were 14000 rpm and 10 min respectively, UV time was 15 min.

The spectrum of the solid residue was compared to that of pristine monomer: C=C stretching at 1635 and 1619  $\text{cm}^{-1}$  was absent in the irradiated sample, whereas the C=O group stretching at 1720  $\text{cm}^{-1}$  was still detected. Such evidences confirmed the effective monomer crosslinking leading to the disappearance of vinyl groups and the creation of a polymer network whose backbone contained carboxy groups.

Dimensional characterization was carried out by means of DLS on polymerized samples. The results are reported in Table 3.

**Table 3.** Nanoparticle average size and PDI as measured by DLS for the UV step study. UT speed and time were 14000 rpm and 10 min respectively for every sample. The adopted formulation was the optimized one.

<i>UV time, min</i>	<i>Z-Average, nm</i>	<i>Std dev, nm</i>	<i>PDI, -</i>
15	116	5.2	0.28
20	107	34.2	0.23
25	146	31.4	0.12

Increasing UV curing time had a major effect on aggregation of the hydrogel nanoparticles. As a matter of fact, the presence of macroscopic aggregates could have been evinced just after the polymerization. Such a behavior was observed for productions exposed 20 min or more to UV radiation. For these samples, DLS measurements were carried out paying attention not to withdraw aggregates from the reactor. However, the significantly higher values of standard deviation for the average size of particle populations evidenced that excessive UV exposures were deleterious for the intra-batch dimensional uniformity. ANOVA evidenced a quasi-significant effect on nanohydrogel size ( $p = 0.063$ ) and a significant effect of irradiation time on PDI ( $P=0.005$ ). This result further corroborates the identification of irradiation time as a relevant process parameter. Therefore, UV irradiation time was set at 15 min for the following part of

the study since it provided the optimal combination among complete monomer conversion, proper formation of the nanohydrogel network and reproducibility.

Lastly, an investigation on the ratio between the dispersed and the continuous phase was carried out. The amount of dispersed phase was varied between 0.25 and 1% relative to the continuous phase. As reported in Table 4, the average size of the nanohydrogel suspension was not significantly affected ( $p = 0.827$ ), contrary to what happened to PDI ( $p = 0.027$ ). However, the picture is a bit more complex. With concentration of dispersed phase up to 0.75%, no effect was observed on PDI ( $p = 0.548$ ). On the other side, when data relative to 1% dispersed phase concentration were included in ANOVA analysis, it was observed that they had a significant different mean. This result suggests that above a threshold value the concentration of dispersed phase played a role on sample polydispersity. Moreover, the volume of the dispersed phase determines the quantity of active principle which can be loaded into the nanohydrogels. Therefore, in order to deal with a system having a significant amount of nanohydrogels and increase the loading of the active principle, 1% of dispersed phase was selected for the following part of the study.

**Table 4.** Nanoparticle average size and PDI as measured by DLS for various percentages of dispersed phase. UT (1400 rpm) and UV times were 10 min and 15 min respectively. All the runs were carried out using the optimized formulation.

<i>Dispersed phase, %</i>	<i>Z-Average, nm</i>	<i>Std dev, nm</i>	<i>PDI, -</i>
0.25	112.6	18.9	0.22
0.5	112.5	10.9	0.19
0.75	109.9	9.8	0.17
1	116.0	5.2	0.28

## *Caffeine payload*

Once the optimal formulation composition had been identified, the loading of the nanocarrier with an active principle was investigated. The model compound was caffeine, which is a rather hydrophilic substance and, therefore, compatible with the nanohydrogel chemical composition. In order to determine the amount of caffeine which could be loaded into the nanocarrier, caffeine solubility in water for injectable preparations was first determined and found to be 26.9 mg/mL at room temperature. It is known that the presence of salts alters caffeine solubility and distribution phenomena in water [44]. In this perspective, water for injections was chosen as the main component of the dispersed phase so as to minimize the effects rising from the variability in ion content of other kinds of water. Successively, caffeine solubility in the dispersed phase was tested. The presence of the monomer and the photoinitiator did not turn out to reduce the amount of caffeine which could be dissolved in the solution. At the end of this preliminary test, the amount of caffeine to be loaded in the carrier was set at 25 mg/mL of dispersed phase. This value guarantees high payload of the active principle and the respect of the solubility limit. Caffeine was loaded in the dispersed phase before the creation of the miniemulsion and successive polymerization. Firstly, the impact of caffeine encapsulation on the nanohydrogel size was investigated by means of DLS. Representative dimensional distributions are reported in Figure 4.

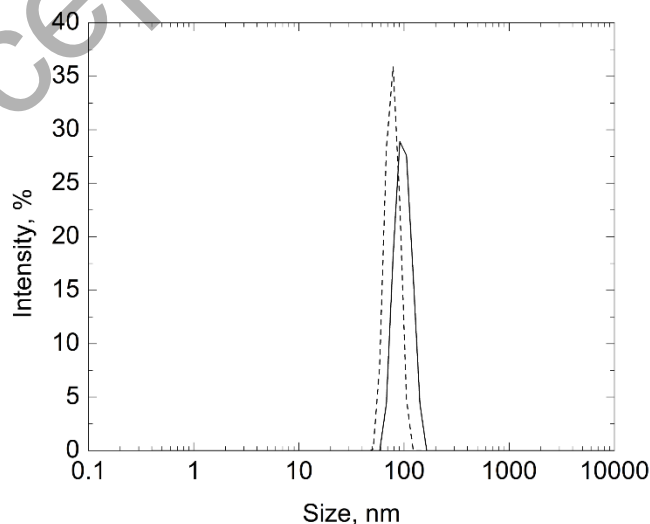


**Figure 4.** Dimensional distribution of the unloaded nanohydrogel population (continuous curve) and nanohydrogels loaded with caffeine (dashed curve). Data refer to the optimized formulation which has been exposed to UV radiation for 15 min. UT was carried out at 14000 rpm for 10 min.

The presence of the active principle did not significantly affect the size of the particles population. The caffeine-loaded nanohydrogel suspension was characterized by the unimodal dimensional distribution centered at 107 nm and a good overlapping between the two distributions was evinced. PDI was 0.2, proving that the addition of caffeine was not deleterious for the system monodispersity. These remarks were corroborated by ANOVA since a significant correlation between caffeine-loaded and unloaded samples was evidenced neither for size ( $p = 0.141$ ) nor PDI ( $p = 0.177$ ). Then, the effect of caffeine incorporation on the monomer conversion was assessed. A DSC scan was performed on the dried solid residue (see Supporting Information, Figure S3). The monomer melting peak was absent, thus suggesting that the presence of the active principle did not disturb the effective crosslinking of PEGDA.

After having assessed the unaltered features of the nanocarrier, the encapsulation efficiency (EE) of our system was evaluated by means of IR investigation. As a matter of fact, the nanohydrogel suspension has been specifically designed for the encapsulation of hydrophilic substances whose solubility in the continuous phase would be extremely low. In particular, since caffeine is insoluble in sunflower oil, it would be confined inside the miniemulsion aqueous droplets. This feature allows one to state that the amount of caffeine loaded inside the carrier is equal to the amount of caffeine initially dissolved inside the dispersed phase. For this purpose, the spectra of pristine caffeine, sunflower oil and supernatant collected after centrifugation are reported in Figure 5.

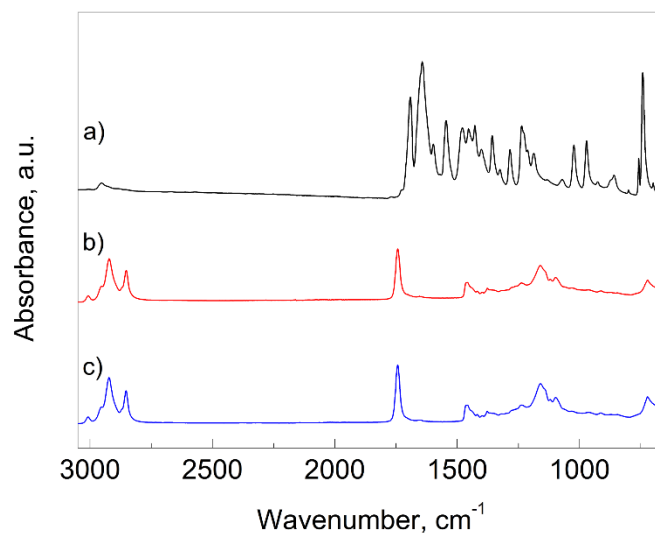


**Figure 5.** FTIR spectra of a) caffeine, b) sunflower oil, c) supernatant separated after centrifugation.

As it can be seen from the graph, no traces of caffeine are visible in the oily residue, thus confirming its absence inside the continuous phase. Caffeine characteristic C=N and C=O peaks between 1700 and 1600  $\text{cm}^{-1}$  were completely absent and the spectrum was identical to that of pristine sunflower oil. These results confirmed the expected encapsulation efficiency of 100%. This finding was corroborated by the IR analysis of a physical mixture of sunflower oil and traces of caffeine (see Figure S4 in Supporting Information). The characteristic peaks of caffeine were detected, thus validating the suitability of this experimental procedure for the evaluation of the active principle encapsulation efficiency. This feature is particularly interesting since it is extremely difficult to get high EEs of caffeine inside nanometric vectors. In conclusion, the caffeine loading did not alter the polymerization step, neither affected the dimensional distribution of the population of particles. The active principle was confined inside the droplets, resulting in unitary EE.

### *In vitro* release study

The optimized formulation including caffeine was finally tested in terms of the active principle release *in vitro*. The final aim of our study was to develop a system which could be suitable for potential application

to transdermal release of therapeutic agents. In this perspective, the formulation was carefully tailored in terms of biocompatibility. The polymeric material is derived from PEGDA and is characterized by a polyether backbone whose compatibility with the human body has been proven. Moreover, such a polymer is non-toxic, poorly immunogenic and biocompatible [45]. The continuous phase consisted of vegetable oil whose ability to act as a permeation enhancer in transdermal formulations has been reported in literature [46,47]. Moreover, our system configuration may enable the overcome of the limitations deriving from the chemical nature of the different layers of skin. As a matter of fact, the lipophilic nature of the formulation would be compatible to that of the first skin layers, thus encouraging its permeation through them. Then, the hydrophilic nature of the carrier would prevail and its affinity with the dermis would guarantee the release of the active principle and its successive migration to the blood circulating system.

The *in vitro* release tests were carried out in dialysis membranes immersed in PBS so as to simulate the pH of blood. Two different systems were tested: the nanohydrogel suspension and a non-polymerized miniemulsion. The latter involved the same synthesis protocol of the optimized nanohydrogel except for the incorporation of monomer and photoinitiator and was used as control to assess the performances of our polymeric nanovectors in terms of release ability and efficiency. Caffeine concentration in the receptor compartment was determined by means of UV/VIS spectrophotometry and the cumulative release curve is plotted in Figure 6 (blue curve). The cumulative mass of caffeine at each time step was calculated as follows:

$$m_{c, \text{caffeine}}(t) = V_{\text{PBS}} C_{\text{caffeine}}(t) + V_{\text{withdrawn}} \sum_{i=0}^{t-1} C_{i, \text{caffeine}} \quad (2)$$

Such values were then divided by the final caffeine concentration in the receptor compartment so as to get the normalized cumulative released mass.

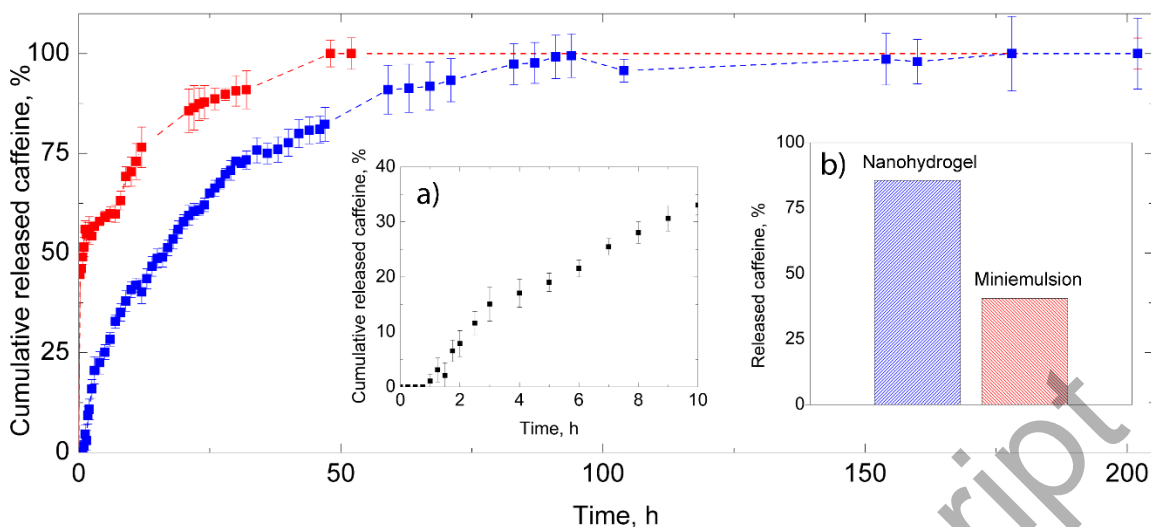


**Figure 6.** Comparison between the normalized cumulative release of caffeine from the nanohydrogel suspension (blue curve) and the miniemulsion (red curve) as a function of time. Scale bars refer to standard deviation calculated from data deriving from three release tests. a) Enlargement of the first 10 hours of the release of caffeine from the nanohydrogels. b) Total amount of the released caffeine from the nanohydrogel suspension and from the miniemulsion.

As regards the nanohydrogel suspension, the caffeine release curve can be divided into three main sections. The first one represents a lag phase, where the active principle is not released (approximately 1 h), as can be seen in inset a) of Figure 6. This behavior was attributed to the time required by the nanohydrogels to diffuse towards the hydrophilic membrane. Once a sufficient number of carriers was located at the interface between the dialysis bag and the oil, the release of caffeine, and thus the second phase, could begin. Such a release appears to be sustained for the first 50 hours, then the curve slope decreases until a plateau is reached after 100 hours. At the end of the test (202 hours), the total amount of caffeine which has been released was found to be 86% with respect to the initial payload of the system.

In order to better understand the phenomena dominating the drug release from the nanostructures, the experimental data were fitted with several well-known mathematical models. Firstly, a fitting based on the Weibull model was performed ( $R^2 = 0.96$ ) and reported in Figure S5. The function turned out to be:

$$F(t) = \begin{cases} 0 & t < 1 \text{ h} \\ 1 - e^{-0.032(t-1)^{1.06}} & t \geq 1 \text{ h} \end{cases} \quad (3)$$

The Weibull model is empirically derived, but can describe the release of a wide variety of drugs from nanoparticles whose rate is governed by dissolution, diffusion and dissolution/diffusion processes [43,48].

The fitting parameter  $b$  turned out to be 1.06, indicating an exponential behavior ( $b = 1$ ).

Experimental data were then fitted according to different kinetic release models in order to investigate the dominant release mechanism.

**Table 5.** Fitting of the experimental data with different kinetic release models.

<i>Kinetic release model</i>	<i>Model equation</i>	$R^2$
Zero Order	$F = k_0 t$	0.96
First Order	$\ln(1-F) = -k_1 t$	0.78
Higuchi	$F = k_H t^{1/2}$	0.99
Hixson-Crowell	$1-(1-F)^{1/3} = k_{HC} t$	0.92
Baker-Lonsdale	$3/2[1 - (1-F)^{2/3}] - F = k_{BL} t$	0.89

The Higuchi model provided the best fitting with experimental values, thus indicating a predominant diffusion-controlled mechanism of release. This evidence turned out to be consistent with the considerations emerged from the Weibull model fitting and allows us to conclude that diffusion across the crosslinked polymeric chains is the dominant phenomenon in controlling the release.

As reference, in the release test, a control sample involving a caffeine-loaded miniemulsion was studied.

This non-encapsulated formulation underwent the release test and was characterized by significantly

different behavior. The red curve in Figure 6 displays an initial burst release of about 20% of caffeine. In the following hours, a further release occurred, making the content of active principle in the receptor fluid to increase. Moreover, the plateau value of the released drug is much higher in the encapsulated system rather than in the caffeine-loaded miniemulsion. We hypothesize that the initial burst release of caffeine from the non-encapsulated formulation is due the formation of a thin water layer at the hydrophilic membrane interface. As a matter of fact, the miniemulsion droplets would be more prone to destabilization rising from the chemical affinity with the membrane and the lack of structural stabilization resulting from photo-crosslinking. Therefore, as soon as they reach the interface, a thin film may be formed and the ensuing caffeine release occurs under the same conditions involved in the release from a caffeine solution. The diffusion of caffeine molecules across the membrane would not represent a rate-limiting step since the increase of drug concentration in the receptor compartment appeared to be instantaneous. Then, the release would be dominated by diffusion of the droplets towards the water film and successive diffusion of caffeine across it. Such a mechanism may be responsible for the gradual release of active principle which has been experimentally observed. Conversely, as far as nanohydrogels are concerned, initial lag followed by gradual release is observed, proving that the polymeric structures are capable of slowing the release kinetics and eluting the drug over a longer period of time.

Concerning the differences in the plateau quantity of released caffeine, some considerations must be done. It is indeed well known that caffeine molecules undergo degradation under UV irradiation. Such an issue is quite common to several drug molecules and sometimes limits the shelf life of pharmaceutical formulations. Given the use of UV light in the synthesis of the nanocarriers, the potential degradation of the caffeine molecules had been initially assessed by spectrophotometry. After UV irradiation of a solution of caffeine, using the same operating conditions used for the encapsulation process, we observed a decrease of about 40% in the absorbance peak at 273 nm. Conversely, when photoinitiator was added to the solution according to the ratios used in the nanohydrogel synthesis, the decrease in caffeine absorbance turned out to be around 1%. Therefore, the photoinitiator had a vital role as concerns the protection of the active ingredient from UV degradation. These results suggest that our encapsulation

process allows the protection of the drug molecule from external factors that could degrade it and is in agreement with the findings of Bazzano *et al.* [49] who successfully employed this approach to incorporate an even more UV-sensitive drug such as curcumin. Instead, the amount of drug released by the caffeine-loaded miniemulsion is lower and this is ascribed to the absence of the photoinitiator in the emulsion and therefore of UV protection.

## CONCLUSIONS

The present study is intended for the synthesis of biocompatible nanohydrogels for the encapsulation of hydrophilic drugs. Caffeine was selected as the model compound because of its chemical nature and therapeutic activity. Firstly, the synthesis has been optimized based on dimensional criteria. The effective monomer crosslinking has been investigated by means of thermal and spectroscopic investigation. Then, the loading of the nanocarrier with the active principle has been assessed. Extremely high encapsulation efficiency was achieved thanks to the confinement of caffeine within the miniemulsion droplets. This feature permitted the exact determination of the initial payload of caffeine into the nanohydrogels. The suspension of nanohydrogels was then tested in terms of its release capability by means of dialysis tests. Caffeine was successfully released from the nanohydrogels, confirming suitability of such a system for controlled and sustained release of drugs. The *ex-vivo* release tests will be discussed in a future study so as to bring the presented nanohydrogel suspension one step closer to the application to transdermal release.

## ASSOCIATED CONTENT

Additional Electronic Supporting Information may be found in the online version of this article.

## AUTHOR INFORMATION

### Corresponding Author

\* e-mail: *roberto.pisano@polito.it*, Tel. +39 011 0904679

### Author Contributions

The manuscript was written through contributions of all authors. All authors have given approval to the final version of the manuscript.

### Funding sources

This research did not receive any specific grant from funding agencies in the public, commercial, or not-for-profit sectors.

## ABBREVIATIONS

ATR, attenuated total reflectance; DLS, dynamic light scattering; EE, encapsulation efficiency; FTIR, Fourier transformed infrared; HLB, hydrophilic lipophilic balance; PDI, polydispersity index; PI, photoinitiator; SDS, sodium dodecyl sulfate; US, ultrasound; UT, Ultra Turrax, UV, ultraviolet.

## NOMENCLATURE

$C_{\text{caffeine}}$ , caffeine concentration;  $\Delta H_m$ , enthalpy of fusion;  $F$ , fraction of caffeine released;  $k_0$ , zero order model constant;  $k_1$ , first order model constant;  $k_H$ , Higuchi model constant;  $k_{HC}$ , Hixson-Crowell model constant;  $k_{BL}$ , Baker-Lonsdale model constant;  $m_{c,\text{caffeine}}$ , cumulative mass of caffeine;  $t$ , time;  $V_{\text{PBS}}$ , volume of the receptor compartment;  $V_{\text{withdrawn}}$ , withdrawn volume.

## REFERENCES

- [1] J.M. Asua, Miniemulsion polymerization, *Prog. Polym. Sci.* 27 (2002) 1283–1346. doi:10.1016/S0079-6700(02)00010-2.
- [2] K. Landfester, Miniemulsions for nanoparticle synthesis, *Top. Curr. Chem.* 227 (2003) 75–123. doi:10.1007/b10835.
- [3] F. Artusio, M. Bazzano, R. Pisano, P.E. Coulon, G. Rizza, T. Schiller, M. Sangermano, Polymeric nanocapsules via interfacial cationic photopolymerization in miniemulsion, *Polym. (United Kingdom)* 139 (2018) 155–162. doi:10.1016/j.polymer.2018.02.019.
- [4] K. Piradashvili, E.M. Alexandrino, F.R. Wurm, K. Landfester, Reactions and polymerizations at the liquid-liquid interface, *Chem. Rev.* 116 (2016) 2141–2169. doi:10.1021/acs.chemrev.5b00567.
- [5] A.S. Hoffman, Hydrogels for biomedical applications, *Adv. Drug Deliv. Rev.* 64 (2012) 18–23. doi:10.1016/j.addr.2012.09.010.
- [6] J. Abedi-Koupai, F. Sohrab, G. Swarbrick, Evaluation of hydrogel application on soil water retention characteristics, *J. Plant Nutr.* 31 (2008) 317–331. doi:10.1080/01904160701853928.
- [7] L. Zheng, Q. Ao, H. Han, X. Zhang, Y. Gong, Evaluation of the chitosan/glycerol- $\beta$ -phosphate disodium salt hydrogel application in peripheral nerve regeneration, *Biomed. Mater.* 5 (2010). doi:10.1088/1748-6041/5/3/035003.
- [8] T.R. Hoare, D.S. Kohane, Hydrogels in drug delivery: Progress and challenges, *Polymer (Guildf)* 49 (2008) 1993–2007. doi:10.1016/j.polymer.2008.01.027.
- [9] K. McAllister, P. Sazani, M. Adam, M.J. Cho, M. Rubinstein, R.J. Samulski, J.M. DeSimone, Polymeric nanogels produced via inverse microemulsion polymerization as potential gene and antisense delivery agents, *J. Am. Chem. Soc.* 124 (2002) 15198–15207. doi:10.1021/ja027759q.
- [10] K. Ganguly, K. Chaturvedi, U.A. More, M.N. Nadagouda, T.M. Aminabhavi, Polysaccharide-based micro/nanohydrogels for delivering macromolecular therapeutics, *J. Control. Release* 193 (2014) 162–173. doi:10.1016/j.jconrel.2014.05.014.
- [11] Y.J. Pan, Y.Y. Chen, D.R. Wang, C. Wei, J. Guo, D.R. Lu, C.C. Chu, C.C. Wang, Redox/pH dual

- stimuli-responsive biodegradable nanohydrogels with varying responses to dithiothreitol and glutathione for controlled drug release, *Biomaterials* 33 (2012) 6570–6579. doi:10.1016/j.biomaterials.2012.05.062.
- [12] M. Hamidi, A. Azadi, P. Rafiei, Hydrogel nanoparticles in drug delivery, *Adv. Drug Deliv. Rev.* 60 (2008) 1638–1649. doi:10.1016/j.addr.2008.08.002.
- [13] M. Shilo, A. Sharon, K. Baranes, M. Motiei, J.P.M. Lellouche, R. Popovtzer, The effect of nanoparticle size on the probability to cross the blood-brain barrier: An in-vitro endothelial cell model, *J. Nanobiotechnology* 13 (2015) 1–7. doi:10.1186/s12951-015-0075-7.
- [14] C.W. Pouton, L.W. Seymour, Key issues in non-viral gene delivery, *Adv. Drug Deliv. Rev.* 46 (2001) 187–203. doi: 10.1016/S0169-409X(00)00133-2.
- [15] G. Sonavane, K. Tomoda, A. Sano, H. Ohshima, H. Terada, K. Makino, In vitro permeation of gold nanoparticles through rat skin and rat intestine: Effect of particle size, *Colloids Surfaces B Biointerfaces* 65 (2008) 1–10. doi:10.1016/j.colsurfb.2008.02.013.
- [16] R. Alvarez-Román, A. Naik, Y.N. Kalia, R.H. Guy, H. Fessi, Skin penetration and distribution of polymeric nanoparticles, *J. Control. Release*. 99 (2004) 53–62. doi:10.1016/j.jconrel.2004.06.015.
- [17] C. Solans, P. Izquierdo, J. Nolla, N. Azemar, M.J. Garcia-Celma, Nano-emulsions, *Curr. Opin. Colloid Interface Sci.* 10 (2005) 102–110. doi:10.1016/j.cocis.2005.06.004.
- [18] A. Chemtob, B. Kunstler, C. Croutxé-Barghorn, S. Fouchard, Photoinduced miniemulsion polymerization, *Colloid Polym. Sci.* 288 (2010) 579–587. doi:10.1007/s00396-010-2190-1.
- [19] F.J. Schork, Y. Luo, W. Smulders, J.P. Russum, A. Butté, K. Fontenot, Miniemulsion polymerization, *Adv. Polym. Sci.* 175 (2005) 129–255. doi:10.1007/b100115.
- [20] M.A. Heckman, J. Weil, E.G. de Mejia, Caffeine (1, 3, 7-trimethylxanthine) in foods: A comprehensive review on consumption, functionality, safety, and regulatory matters, *J. Food Sci.* 75 (2010) 77–87. doi:10.1111/j.1750-3841.2010.01561.x.
- [21] J.A. E.R. Goldstein, T. Ziegenfuss, D. Kalman, R. Kreider, B. Campbell, C. Wilborn, L. Taylor, D. Willoughby, J. Stout, B.S. Graves, R. Wildman, J.L. Ivy, M. Spano, A.E. Smith, International

- society of sports nutrition position stand: Caffeine and performance, *J. Int. Soc. Sports Nutr.* 7 (2010) 1–15. doi:10.1186/1550-2783-7-5.
- [22] B. Schmidt, R.S. Roberts, P. Davis, L.W. Doyle, K.J. Barrington, A. Ohlsson, A. Solimano, W. Tin, Long-term effects of caffeine therapy for apnea of prematurity, *N. Eng. J. Med.* 357 (2007) 1893–1902. doi:10.1056/NEJMoa1414264.
- [23] T.P.A. Devasagayam, J.P. Kamat, H. Mohan, P.C. Kesavan, Caffeine as an antioxidant: Inhibition of lipid peroxidation induced by reactive oxygen species, *Biochim. Biophys. Acta.* 1282 (1996) 63–70. doi:10.1016/S0300-483X(03)00149-5.
- [24] Y.P. Lu, Y.R. Lou, J.G. Xie, Q.Y. Peng, S. Zhou, Y. Lin, W.J. Shih, A.H. Conney, Caffeine and caffeine sodium benzoate have a sunscreen effect, enhance UVB-induced apoptosis, and inhibit UVB-induced skin carcinogenesis in SKH-1 mice, *Carcinogenesis* 28 (2007) 199–206. doi:10.1093/carcin/bgl112.
- [25] S.W. Koo, S. Hirakawa, S. Fujii, M. Kawasumi, P. Nghiem, Protection from photodamage by topical application of caffeine after ultraviolet irradiation, *Br. J. Dermatol.* 156 (2007) 957–964. doi:10.1111/j.1365-2133.2007.07812.x.
- [26] Y.-P. Lu, Y.-R. Lou, Y. Lin, W.J. Shih, M.-T. Huang, C.S. Yang, A.H. Conney, Inhibitory effects of orally administered green tea, black tea, and caffeine on skin carcinogenesis in mice previously treated with ultraviolet B light (high-risk mice): Relationship to decreased tissue fat, *Cancer Res.* 61 (2001) 5002–5009.
- [27] G. Ginsberg, D. Hattis, A. Russ, B. Sonawane, Physiologically based pharmacokinetic (PBPK) modeling of caffeine and theophylline in neonates and adults: Implications for assessing children's risks from environmental agents, *J. Toxicol. Environ. Heal. - Part A.* 67 (2004) 297–329. doi:10.1080/15287390490273550.
- [28] P. Nawrot, S. Jordan, J. Eastwood, J. Rotstein, A. Hugenholtz, M. Feeley, Effects of caffeine on human health, *Food Addit. Contam.* 20 (2003) 1–30. doi:10.1080/0265203021000007840.
- [29] M. Dias, A. Farinha, E. Faustino, J. Hadgraft, J. Pais, C. Toscano, Topical delivery of caffeine

- from some commercial formulations, *Int. J. Pharm.* 182 (1999) 41–47. doi:10.1016/S0378-5173(99)00067-8.
- [30] G. Cevc, U. Vierl, Nanotechnology and the transdermal route: A state of the art review and critical appraisal, *J. Control. Release.* 141 (2010) 277–299. doi:10.1016/j.jconrel.2009.10.016.
- [31] C. Kim, J. Shim, S. Han, I. Chang, The skin-permeation-enhancing effect of phosphatidylcholine: caffeine as a model active ingredient., *J. Cosmet. Sci.* 53 (2002) 363–374.
- [32] M.J. Santander-Ortega, T. Stauner, B. Loretz, J.L. Ortega-Vinuesa, D. Bastos-González, G. Wenz, U.F. Schaefer, C.M. Lehr, Nanoparticles made from novel starch derivatives for transdermal drug delivery, *J. Control. Release.* 141 (2010) 85–92. doi:10.1016/j.jconrel.2009.08.012.
- [33] C. Puglia, A. Offerta, G.G. Tirendi, M.S. Tarico, S. Curreri, F. Bonina, R.E. Perrotta, Design of solid lipid nanoparticles for caffeine topical administration, *Drug Deliv.* 23 (2016) 36–40. doi:10.3109/10717544.2014.903011.
- [34] A.I. Bourbon, M.A. Cerqueira, Encapsulation and controlled release of bioactive compounds in lactoferrin-glycomacropptide nanohydrogels: Curcumin and caffeine as model compounds, *J. Food Eng.* 180 (2016) 110–119. doi:10.1016/j.jfoodeng.2016.02.016.
- [35] M.A. Bolzinger, S. Briançon, J. Pelletier, H. Fessi, Y. Chevalier, Percutaneous release of caffeine from microemulsion, emulsion and gel dosage forms, *Eur. J. Pharm. Biopharm.* 68 (2008) 446–451. doi:10.1016/j.ejpb.2007.10.018.
- [36] D. Massella, E. Celasco, F. Salaün, A. Ferri, A. Barresi, Overcoming the limits of flash nanoprecipitation: Effective loading of hydrophilic drug into polymeric nanoparticles with controlled structure, *Polymers (Basel)* 10 (2018) 1092. doi:10.3390/polym10101092.
- [37] D. Massella, F. Leone, R. Peila, A. Barresi, A. Ferri, Functionalization of cotton fabrics with polycaprolactone nanoparticles for transdermal release of melatonin, *J. Funct. Biomater.* 9 (2017) 1. doi:10.3390/jfb9010001.
- [38] A.M. Nikoo, R. Kadkhodae, B. Ghorani, H. Razzaq, N. Tucker, Electrospray-assisted encapsulation of caffeine in alginate microhydrogels, *Int. J. Biol. Macromol.* 116 (2018) 208–216.

- doi:10.1016/j.ijbiomac.2018.04.167.
- [39] L. Bagheri, A. Madadlou, M. Yarmand, M.E. Mousavi, Spray-dried alginate microparticles carrying caffeine-loaded and potentially bioactive nanoparticles, *Food Res. Int.* 62 (2014) 1113–1119. doi:10.1016/j.foodres.2014.05.040.
- [40] N. Mohammadi, M.R. Ehsani, H. Bakhoda, Design and evaluation of the release characteristics of caffeine-loaded microcapsules in a medicated chewing gum formulation, *Food Biophys.* 13 (2018) 240–249. doi:10.1007/s11483-018-9530-y.
- [41] N. Noor, A. Shah, A. Gani, A. Gani, F.A. Masoodi, Microencapsulation of caffeine loaded in polysaccharide based delivery systems, *Food Hydrocoll.* 82 (2018) 312–321. doi:10.1016/j.foodhyd.2018.04.001.
- [42] P. Khazaeli, A. Pardakhty, H. Shoorabi, Caffeine-loaded niosomes: Characterization and in vitro release studies, *Drug Deliv.* 14 (2007) 447–452. doi:10.1080/10717540701603597.
- [43] V. Papadopoulou, K. Kosmidis, M. Vlachou, P. Macheras, On the use of the Weibull function for the discernment of drug release mechanisms, *Int. J. Pharm.* 309 (2006) 44–50. doi:10.1016/j.ijpharm.2005.10.044.
- [44] A. Al-Maaieh, D.R. Flanagan, Salt effects on caffeine solubility, distribution, and self-association, *J. Pharm. Sci.* 91 (2002) 1000–1008. doi:10.1002/jps.10046.
- [45] S. Nemir, H.N. Hayenga, J.L. West, PEGDA hydrogels with patterned elasticity: Novel tools for the study of cell response to substrate rigidity, *Biotechnol. Bioeng.* 105 (2010) 636–644. doi:10.1002/bit.22574.
- [46] H.R. Patel, R.B. Patel, G.N. Patel, M.M. Patel, The influence and compatibility of vegetable oils and other additives on release of ketoprofen from transdermal films, *East Cent. African J. Pharm. Sci.* 13 (2010) 19–24. doi:10.1016/j.foodchem.2011.05.115.
- [47] A. Kumar, G. Aggarwal, K. Singh, S.L. Harikumar, Comparison of vegetable and volatile oils as skin permeation enhancers for transdermal delivery of losartan potassium, *Der Pharm. Lett.* 6 (2014) 199–213.

- [48] M. Barzegar-Jalali, K. Adibkia, H. Valizadeh, M.R.S. Shadbad, A. Nokhodchi, Y. Omid, G. Mohammadi, S.H. Nezhadi, M. Hasan, M. Reza, S. Shadbad, Kinetic analysis of drug release from nanoparticles, *J. Pharm. Pharm. Sci.* 11 (2008) 167–177.
- [49] M. Bazzano, R. Pisano, J. Brelstaff, M.G. Spillantini, M. Sidoryk-Wegrzynowicz, G. Rizza, M. Sangermano, Synthesis of polymeric nanocapsules by radical UV-activated interface-emulsion polymerization, *J. Polym. Sci. Part A Polym. Chem.* 54 (2016) 3357–3369. doi:10.1002/pola.28226.

#### GRAPHICAL ABSTRACT

